PISTORIUS, P.C. Ilmenite smelting: the basics. *The 6th International Heavy Minerals Conference 'Back to Basics'*, The Southern African Institute of Mining and Metallurgy, 2007.

Ilmenite smelting: the basics

P.C. PISTORIUS
Department of Materials Science and Metallurgical Engineering, University of Pretoria, Pretoria

While some of the practical details of ilmenite smelting are not well documented, there is a substantial body of literature on the principles of ilmenite smelting, and the behaviour of solidified titania slag. This information is summarized, focusing on the basic reactions, departure from equilibrium, the behaviour of impurities, and reactions of solidified slag. The emphasis is on the South African operations.

Basic reactions

This paper briefly reviews the principles of the ilmenite smelting process. Ilmenite has the nominal composition $FeO.TiO_2$. South African beach-sand ilmenites are close to this nominal composition, with the main impurities being MnO, MgO, SiO_2 and Al_2O_3 (amounting to some 3% of the mass of the ilmenite).

There are two main routes that are used to upgrade ilmenite, to serve as a feedstock for the production of TiO_2 pigment.[1] The pigment is produced mainly via the chloride route. Part of this route involves chlorination of the feedstock in a fluidized bed, to yield volatile chlorides as products. These chlorides are then separated by selective distillation, to yield pure $TiCl_4$ which is then processed further to form pure TiO_2.

The two main routes to upgrade ilmenite to chlorination feedstock are ilmenite smelting, and the synthetic rutile route. Synthetic rutile is produced by solid-state reactions; for example, in the Becher process (as practised widely in Australia) ilmenite is reduced to a mixture of metallic iron and rutile; the iron is then removed by leaching.

In ilmenite smelting, the iron content of the oxide is also lowered by reduction to metallic iron, but this takes place in the liquid state, at a much higher temperature (of around 1650°C). Ilmenite smelting thus yields two products: a titania-rich slag, and molten iron. This is in contrast with the Becher process, where the iron is removed as a waste product. Ilmenite smelting as practised in South Africa (at Richards Bay Minerals, Namakwa Sands, and Exxaro KZN Sands) uses an electric furnace (AC or DC) to provide the required energy input.

The two basic reactions in ilmenite smelting are the following:

Reduction of FeO from the slag:

$$FeO + C \rightarrow Fe + CO \qquad [1]$$

Partial reduction of TiO_2 in the slag:

$$TiO_2 + \tfrac{1}{2}C \rightarrow TiO_{1.5} + \tfrac{1}{2}CO \qquad [2]$$

Reaction [1] proceeds further to the right during ilmenite smelting than reaction [2]; possible reasons for this are considered later. The net effect of the balance between these two reactions is that the composition of the molten slag remains close to M_3O_5 stoichiometry[2,3]—the slag can be viewed as a molten mixture of Ti_3O_5, $FeTi_2O_5$, $MnTi_2O_5$, Al_2TiO_5, $MgTi_2O_5$, V_2TiO_5 and Cr_2TiO_5. The solidified slag is then a largely single-phase material (with this phase being the pseudobrookite—M_3O_5—phase, also known as 'karrooite'[3]), with only small proportions of other phases (mainly rutile, and silicates).

These reactions proceed at high temperature, because the high-titania slag has a high melting point (around 1650°C). The exact liquidus relationship in this system is not known, but a calculated diagram is shown in Figure 1 a). This diagram serves to illustrate that both FeO and $TiO_{1.5}$ serve to flux TiO_2, lowering the liquidus temperature of the slag. For slags that lie along the $FeTi_2O_5$-Ti_3O_5 join (line C in Figure 1), calculated liquidus and solidus temperatures are shown in Figure 1 (b). Note the very narrow (predicted) liquidus-solidus gap, of 20–30°C.

Constraints in ilmenite smelting

Several constraints limit the operating ranges of ilmenite smelters. One of the major constraints is on the slag composition. The reason for this is that the chlorination process can handle only low levels of impurities (Table I),

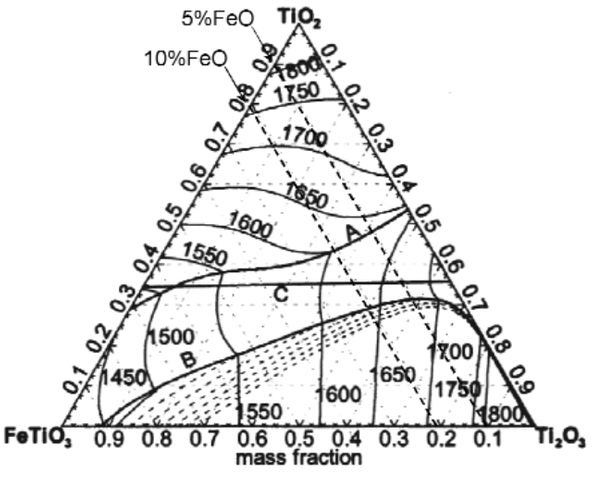

Figure 1 (a). Calculated liquidus diagram of ilmenite smelter slags[4]. Compositions are plotted as mass fractions, and temperatures are in °C. Note that this diagram is for slags that contain only FeO, TiO_2 and Ti_2O_3. Real slag compositions lie just above line C, which traces the compositions of the M_3O_5 (pseudobrookite) solid solutions

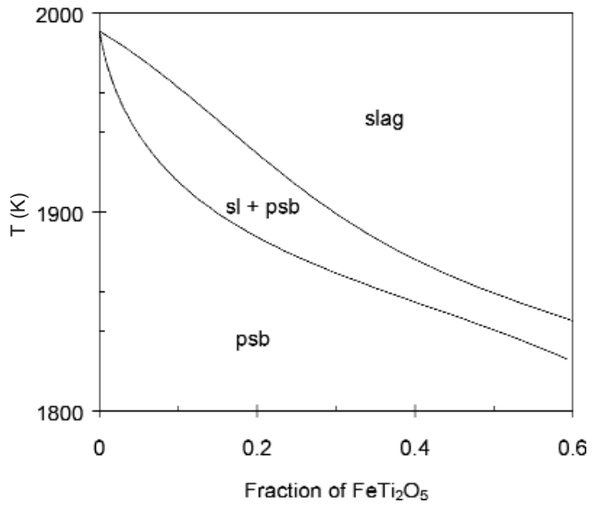

Figure 1 (b). Liquidus and solidus temperatures along the Ti_3O_5-$FeTi_2O_5$ join. The composition is plotted as the mole fraction of $FeTi_2O_5$ in the pseudobrookite solid solution.[5] 10% FeO corresponds to an $FeTi_2O_5$ mole fraction of 0.32. Abbreviations: sl—slag; psb—pseudobrookite

Table I
Typical specification of slag used in the chloride process (mass percentages)

Total $\%TiO_2$	>85.0
$\%Ti_2O_3$	<35.0
%FeO	<12.0
$\%SiO_2$	<2.0
$\%Al_2O_3$	<1.5
%CaO	<0.13
%MgO	<1.2
%MnO	<2.0
$\%Cr_2O_3$	<0.25
$\%V_2O_5$	<0.60

mainly because of the effect of impurities such as MgO and CaO on the stability of the fluidized bed: the boiling points of $MgCl_2$ and $CaCl_2$ (the reaction products of MgO and CaO during chlorination) are above the chlorination temperature—so these chlorides accumulate in the fluidized bed. The strict specifications on impurities imply that no fluxing additions can be made, and that impurity levels in the reductant need to be limited.

The second major constraint is on the balance between the main process inputs, namely power, ilmenite feed rate, and reductant feed rate. In the ilmenite smelter, composition and temperature cannot be controlled independently. The reason for this is that the furnace operates with a 'freeze lining' of solidified slag against this furnace wall. This solidified slag serves to contain the molten slag, and is used because of the aggressive nature of the titania slag towards conventional refractories. Because the smelter operates with liquid slag in contact with solidified slag, and because the slag layer is expected to be well mixed, the slag temperature is expected to remain close to the melting point (liquidus temperature) of the slag. In addition, the slag composition remains close to M_3O_5 stoichiometry. As Figure 1 shows, the effect is that slag composition and temperature are strongly linked, and cannot be separated—at least under steady-state conditions.

The implication of this for controlling the process inputs is illustrated by Figure 2, which summarizes the result of mass and energy balances for ilmenite smelting (based on one of the local ilmenites). The enthalpy expression for the slag that was used in this calculation has been given elsewhere[6]. The figure has important implications for the way in which process inputs need to be changed relative to existing set points, if stable operation is to be maintained: For every 1 MWh change in electrical energy input, the carbon input needs to be changed by 186 kg; put another way, this means that for every 5.3 kWh increase in electrical energy input, the carbon input needs to be increased by 1 kg. It is emphasized that these values are based on theoretical calculations, but similar values are expected for actual furnace operations; the ratio of approximately 5.3 kWh per kg of carbon has also been confirmed with a more comprehensive furnace model[7].

Note also how very sensitive the FeO content of the slag is to changes in the energy input: a change in 10 kWh/ton (i.e. 1% of typical energy input) causes a change in FeO content of 1%. Much of the reason for this sensitivity is that a large part of the energy requirement is consumed by heating the feed material: based on published enthalpy correlations[8], it can be calculated that heating 1 ton of pure ilmenite and 100 kg of carbon to 1600°C requires some 640 kWh per ton of ilmenite. Hence the energy required for the reduction reactions is only about a third of the total energy requirement. The resulting sensitivity of the process to changes in inputs is the likely reason behind the reported decision by Namakwa Sands to discontinue preheating of the ilmenite feed—whereas the preheaters at Namakwa had the ability to preheat the ilmenite feed to 880°C, these were found to have 'severe destabilizing effects' on the furnaces, and both preheat plants at Namakwa were shut down in June 2003[9].

A simple energy balance calculation indicates that, if half the ilmenite feed is preheated to 880°C without any oxidation of the feed, the required energy input is decreased by more than 10%. If a constant degree of preheating can be achieved, this energy saving brings a significant productivity advantage. However, if the actual degree of preheating varies, this has the effect of moving both lines in

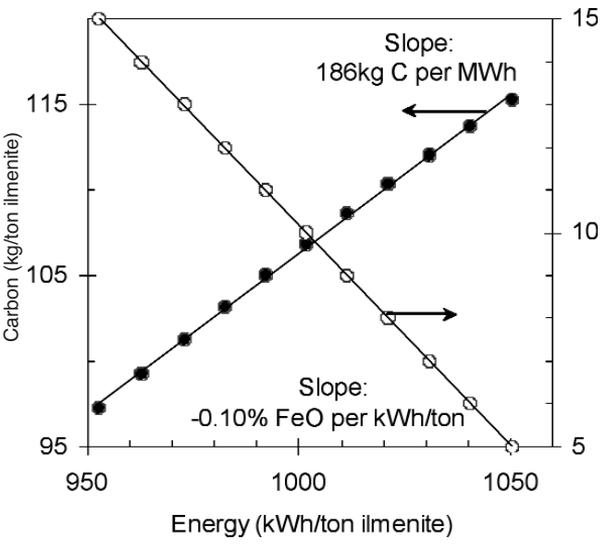

Figure 2. Required carbon input and resulting (%FeO) in ilmenite smelter slag, for steady-state operation and for slag compositions remaining close to stoichiometric M_3O_5

Figure 2 parallel to the *x* axis—which can result in an imbalance between carbon and power inputs, and variable slag grade (% FeO).

This same strict link between inputs of electrical energy and reductant holds under dynamic conditions, for example when the FeO content of the slag is being increased or decreased. Calculated changes in required inputs for such changes are shown in Figure 3. For more rapid changes in FeO content (towards the left in the figure), the offsets in energy and carbon inputs (relative to the original steady-state value) need to be larger, as expected—but the ratio of approximately 5 kWh of (changed) energy input per 1 kg of (changed) carbon input also holds under these conditions.

If the energy and carbon inputs are not matched, the process is destabilized. For example, insufficient carbon input (which implies excessive energy input) will cause the freeze lining to be melted away. An extreme version of this is illustrated in Figure 4, which shows the (calculated) rapid loss in freeze lining if power input into the furnace is maintained, without any reductant input. Note that growth of the freeze lining is much slower than loss of the freeze lining if power input is maintained without any feed—this is because the heat losses through the side wall are much smaller than the power input into the furnace.

If the energy input is too small for the amount of carbon fed, partial solidification of the slag is expected. This may either cause the freeze lining to grow, or can result in the precipitation of solid pseudobrookite in the slag. The latter effect can give rise to uncontrolled slag foaming, because of the sharp increase in the apparent viscosity of ilmenite smelter slags, just below their liquidus—see Figure 5. This sharp increase in apparent viscosity for a small decrease in temperature is consistent with the predicted small liquidus-solidus gap—see Figure 1.

Equilibria and departure from equilibrium in ilmenite smelting

Ilmenite smelting is characterized by departure from equilibrium in several ways:

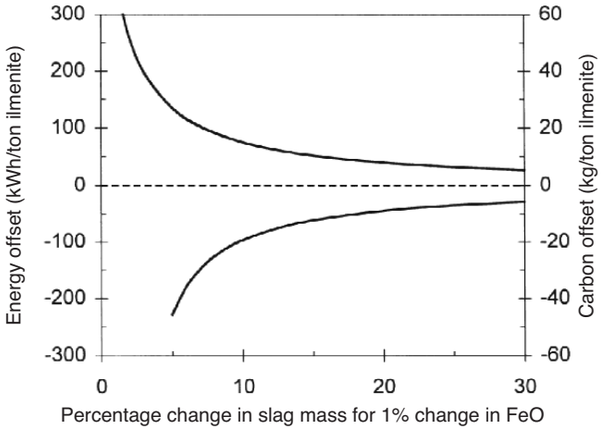

Figure 3. Required average difference between the energy and carbon inputs during a decrease in FeO content (upper half of figure), and an increase in FeO (lower half of figure), as functions of the relative change in slag mass per one per cent change in FeO content[10]. The curves for energy and carbon inputs are exactly superimposed, for a ratio of 5 kWh of energy to 1 kg of carbon

Thermal non-equilibrium

The metal in the smelter is significantly colder than the slag—typically by some 150°C. This means that the metal is at a temperature lower than the melting point of the slag. Partial solidification of the slag at the contact with the metal is hence expected. It is not clear what effect this has on furnace operation—but the temperature difference between metal and slag is the suggested origin of the slag composition relationship (i.e. M_3O_5 stoichiometry)[4], as discussed below in the section on 'reaction mechanisms'.

There is another important departure from thermal equilibrium in the smelter, which is the formation of a freeze lining on the furnace wall where it is in contact with the slag. This serves to protect the furnace lining; if the freeze lining were not present, the slag would tend to attack the lining by dissolution. As examples of the expected interaction, Figure 6 shows the predicted equilibrium phases for reaction of different proportions of refractory and smelter slag, for a high-alumina material, and for magnesia material. The magnesia material is clearly more suitable, since it forms a solid Mg_2TiO_4 (spinel) product—in contrast with the high-alumina material, with liquid formation for even very low ratios of slag to refractory: the

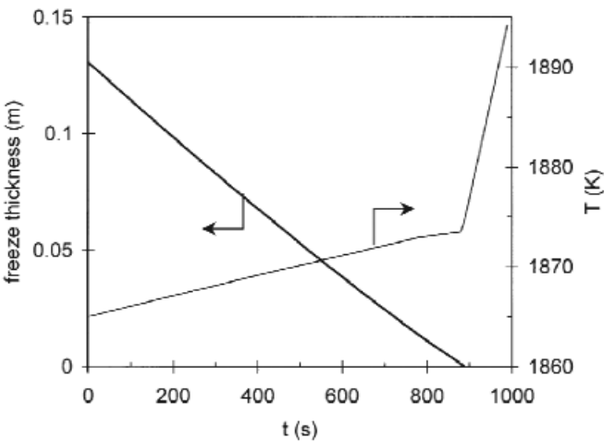

Figure 4. Calculated response of freeze lining thickness and furnace temperature (*T*), if no ilmenite is fed to the furnace, and the furnace power is maintained[6]

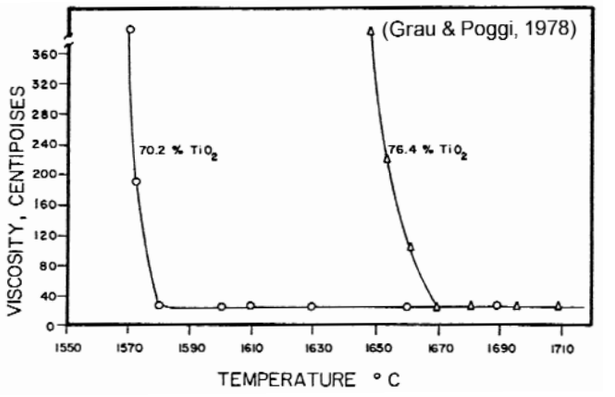

Figure 5. Change in viscosity of QIT slags with temperature; the sharp increase in viscosity at lower temperatures is the result of partial solidification[11]

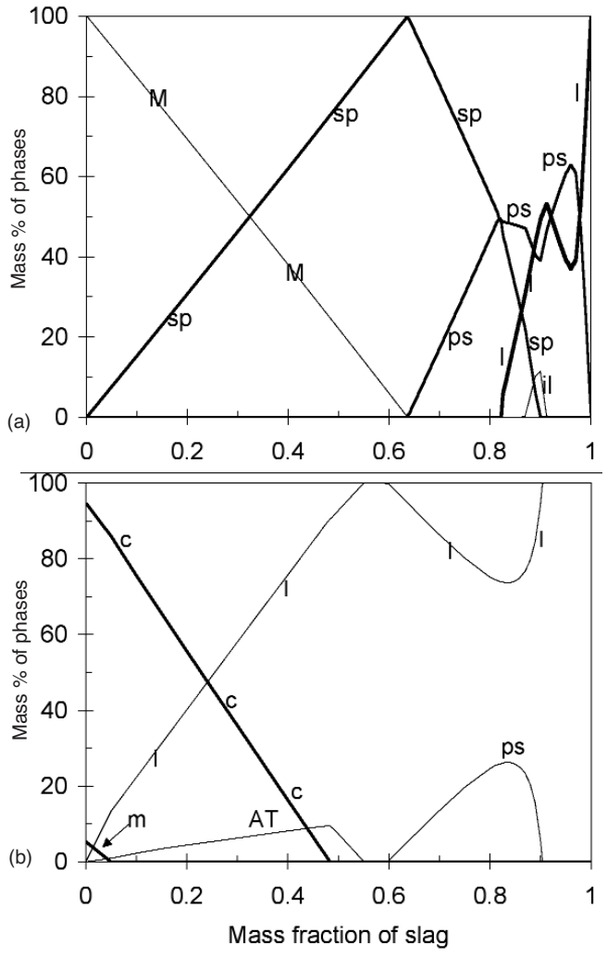

Figure 6. Predicted phase composition after reaction of (a) pure MgO and (b) high-alumina material (98.5 mass% Al_2O_3-1.5 mass%) with different proportions of ilmenite smelter slag (54.4 mass%TiO_2—33.7mass% Ti_2O_3—9.7mass% FeO—1.2 mass% MgO—1.2 mass% MnO) at 1660°C. 'M' is periclase (MgO), 'sp' is spinel $(Al,Mg,Mn,Fe,Ti)_3O_4$, 'ps' pseudobrookite $(Mg,Fe,Mn,Ti)_3O_5$, 'il' ilmenite $(Mg,Mn,Fe,Ti)_2O_3$, 'l' is liquid slag, 'c' is corundum (Al_2O_3), 'm' is mullite, and AT is tialite (Al_2TiO_5). Calculated using FactSage[12]

solidus temperature of the combination of slag and high-alumina refractory is below the assumed temperature of 1660°C. Even the relatively resistant behaviour of the magnesia material is not sufficient in practical smelters, because of the very strict limitation on the allowable MgO content in the slag product (see Table I). This highlights the need for a freeze lining.

Chemical non-equilibrium

The relative abundance of several pairs of species in the furnace is sensitive to how oxidizing or reducing conditions are. Three examples of such pairs are Fe/FeO, $TiO_{1.5}/TiO_2$, and C/CO. In each of the three pairs listed here, the species named first is favoured by more strongly reducing conditions, and the second by less strongly reducing conditions. Hence, if conditions are more strongly reducing, a lower FeO activity and a higher $TiO_{1.5}$ activity are expected in the slag, and a higher carbon activity in the metal.

It can be tested whether these pairs are in mutual equilibrium, by writing the coupled reactions, for example:

$$Fe + 2TiO_2 = FeO + Ti_2O_3 \quad [3]$$

Another way to consider possible coupling of the reactions is by comparing the oxygen activity where each pair would be in equilibrium; examples of such reactions are:

$$Fe + \tfrac{1}{2}O_2 = FeO \quad [4a]$$

$$Ti_2O_3 + \tfrac{1}{2}O_2 = 2TiO_2 \quad [4b]$$

$$C + \tfrac{1}{2}O_2 = CO \quad [4c]$$

Both ways of comparing these possible equilibria (Reactions [3] and [4]) show mutual non-equilibrium between the species. For example, Figure 7 compares the relationship between the FeO and Ti_2O_3 contents of the slags with the equilibrium relationship, which can be predicted by considering the equilibrium constant of reaction [3], and the activities in the slag (calculated using the available quasichemical model). Clearly, the actual slags lie at lower Ti_2O_3 and FeO levels than equilibrium (i.e. Reaction [3] is out of equilibrium to the left). This is a favourable departure from equilibrium: the aim of ilmenite smelting is to reduce FeO to Fe, and this proceeds to a greater extent than the (endothermic and carbon-consuming) side reaction of reduction of TiO_2 to Ti_2O_3. This can be shown in another way, by comparing the oxygen activities, which would be in equilibrium with the three pairs of species shown in Equation [4 a–c]. Such calculated values are shown in Figure 8, together with measured oxygen activity (as measured in the Exxaro pilot smelter).

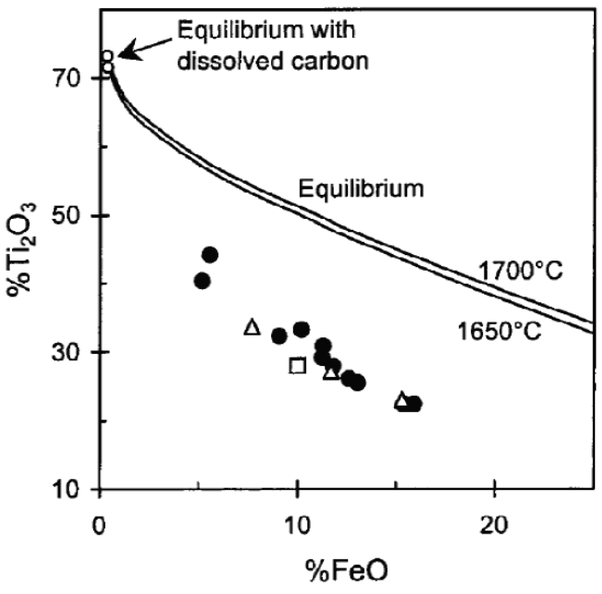

Figure 7. Calculated relationship between FeO and Ti_2O_3 (mass percentages) in pure FeO-TiO_2-$TiO_{1.5}$ slags in equilibrium with pure liquid iron (lines) and liquid iron containing 2% C under an atmosphere with p_{CO}=1 atm (o), compared with the real FeO-Ti_2O_3 trend.[2] Filled circles are for the Exxaro pilot-plant smelter, triangles for RBM, and the square for Namakwa Sands

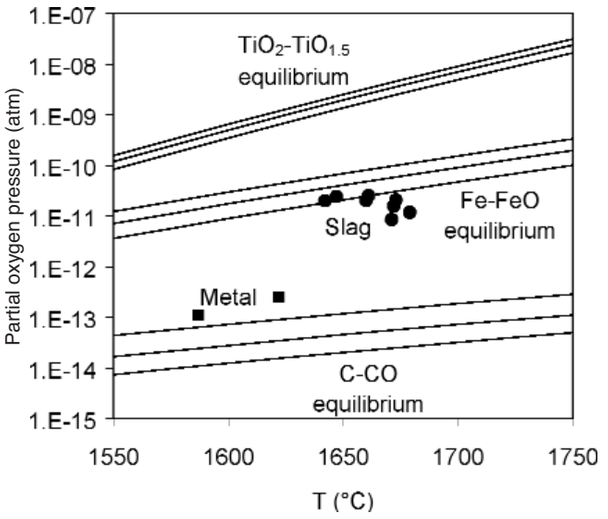

Figure 8. Comparison of the measured partial oxygen pressure in the Exxaro 3MVA pilot-scale ilmenite smelter, with the calculated partial oxygen pressure if fixed by respectively the $TiO_2/TiO_{1.5}$ equilibrium (for slags containing 25%, 30% and 35%$TiO_{1.5}$ respectively, from top to bottom, at constant FeO of 12%), the Fe/FeO equilibrium (for slags containing 15%, 12% and 9%FeO respectively, from top to bottom, at a constant %$TiO_{1.5}$ of 30%), and the C/CO equilibrium (for metal containing 1.5%, 2% and 2.5% C respectively, from top to bottom, with pure CO in the gas phase)[14]

It should also be noted in Figure 8 that the oxygen activity in equilibrium with the dissolved carbon in the metal (typically 2% carbon) and with CO (at p_{CO} = 1 atm) is much lower than for the other two couples. This implies that the FeO content of smelter slag would be much lower if equilibrium with the metal product were reached; this is also illustrated by Figure 7. Another way of viewing this is that the carbon content of the iron in equilibrium with FeO in ilmenite smelter slag is much lower than the actually observed carbon level; this equilibrium carbon content is approximately 0.2%, or a factor ten smaller than the observed carbon content.

The large difference in oxygen activity, for oxygen activities fixed by the Fe/FeO, Ti_2O_3/TiO_2 and C/CO pairs makes it impossible to predict the 'equilibrium' distribution coefficients. For example, in the case of vanadium the practical distribution coefficient which is observed is $(\%V_2O_5)_{slag}/[\%V]_{metal} \approx 20^*$ which is approximately what would be expected if the oxygen activity were fixed by the Ti_2O_3/TiO_2 pair.

This uncertainty means that distribution of species such as Mn, Cr, S and P between metal and slag in the ilmenite smelter cannot be predicted with any certainty—the only broad guideline is that manganese, chromium and phosphorus are expected to partition to the slag to a greater extent under more oxidizing conditions (i.e. with a higher FeO content in the slag), whereas sulphur is expected to partition to the slag to a smaller extent if the FeO content of the slag is higher. However, both sulphur and phosphorus are expected to partition to the metal preferentially.

*Note that the vanadium is expected to be present as V_2O_3 in the slag, not as V_2O_5, but it is expressed as an equivalent amount of V_2O_5 for consistency with the way in which slag analyses are generally reported

Note that Rosenqvist suggested that the slag composition for equilibrium of Reaction [3] in fact lies close to M_3O_5 stoichiometry, in contrast with the predictions shown in Figure 7.[15] If this is the case, the implication is that the slag composition does not depart from slag-metal equilibrium. However, this suggestion does not agree with the FactSage predictions, nor with the experimental data of Pesl and Eriç.[16] It is hence seen as likely that the slag and metal are not in equilibrium.

Behaviour of other impurities in the ilmenite smelter

With the exception of sulphur and phosphorus, most impurities in the ilmenite, and the ash in the reductant, are expected to report to the slag phase. This means that the slag purity is controlled by ilmenite (and reductant) purity, and that there is little or no scope to decrease impurity levels in the smelter. Given that the impurities make up some 3% of the ilmenite, these should then be present at 5–6% in the product. This is indeed what is found—see Figure 9.

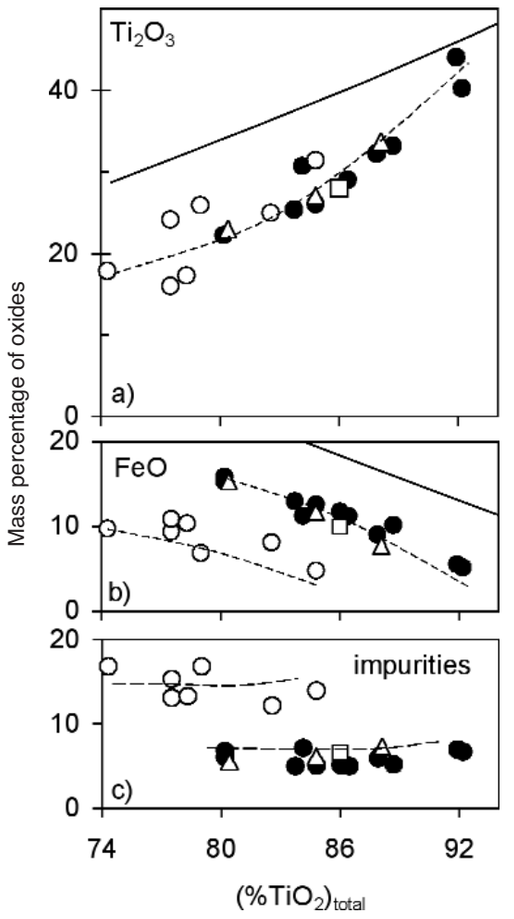

Figure 9. Changes in FeO, Ti_2O_3 and impurity oxide content with increased equivalent total TiO_2 content, for slag produced from Canadian ilmenite (open circles) and South African ilmenite (others). Solid lines in (a) and (b) given calculated relationship for pure FeO-Ti_2O_3-TiO_2 slag in equilibrium with pure liquid iron at 1650°C. Symbols: • Exxaro pilot plant, Δ Richards Bay Minerals, □ Namakwa Sands[2]

Aspects of the reaction mechanisms

Many details of the reaction mechanism within the smelter remain unknown. However, any proposed mechanism needs to explain or at least include several important features, which include the temperature difference between slag and metal, the large departure from equilibrium, the remarkably consistent relationship between the FeO and Ti_2O_3 contents of the slag (see Figure 9), and the density difference between the reductant and the slag.

The relationship between FeO and Ti_2O_3 is such that the composition of the slag follows M_3O_5 stoichiometry. This means that the slag composition can be represented as $[(FeO,MgO,MnO).2(TiO_2)]_x.[(Ti_2O_3,Cr_2O_3,V_2O_3,Al_2O_3).(TiO_2)]_y$—that is, each divalent cation (Fe^{2+}, Mg^{2+} and Mn^{2+}) is associated with two tetravalent Ti^{4+} cations in the slag, and each pair of trivalent cations (Ti^{3+}, Cr^{3+}, V^{3+}, Al^{3+}) is associated with one tetravalent Ti^{4+} cation in the slag. There are several ways to test whether the slag composition does obey this precise relationship; one is to calculate the equivalent FeO content of the slag (the sum of all divalent oxides except CaO, expressed as a corresponding number of moles of FeO), and the equivalent Ti_2O_3 content (the sum of all trivalent oxides, expressed as a corresponding number of moles of Ti_2O_3). The corresponding expressions are:

The equivalent FeO content is:

$$(\%FeO)_{eq} = (\%FeO) + (M_{FeO}/M_{MgO})(\%MgO) + (M_{FeO}/M_{MnO})(\%MnO) \quad [5a]$$

where M_i is the molar mass of oxide $_i$, and the amounts of the oxides are in mass percentages.

Similarly, the equivalent Ti_2O_3 content is:

$$(\%Ti_2O_3)_{eq} = (\%Ti_2O_3) + (M_{Ti_2O_3}/M_{V_2O_5})(\%V_2O_5) + (M_{Ti_2O_3}/M_{Cr_2O_3})(\%Cr_2O_3) + (M_{Ti_2O_3}/M_{Al_2O_3})[\%Al_2O_3 - (\%SiO_2)/3] \quad [5b]$$

In Expression (5b), the vanadium content of slag is expressed as V_2O_5 since this is the convention for the analyses, although the vanadium is expected to be present in the trivalent form. As the expression shows, part of the Al_2O_3 is not taken into account when the equivalent Ti_2O_3 content is calculated, because some Al_2O_3 (a mass taken to be one-third of that of the silica) reports to the separate silicate phases. (CaO and SiO_2 are not included in this calculation, since these report to the silicate phases, and do not dissolve in the solid M_3O_5.)

The sum of $(\%FeO)_{eq}$, $(\%Ti_2O_3)_{eq}$ and $(\%TiO_2)$ is then normalized to 100%, where $(\%TiO_2)$ is the Ti^{4+} content of the slag, expressed as a mass of TiO_2.

The result of this calculation, for literature values of ilmenite smelter slag compositions, is given in Figure 10. Remarkably, all the slags follow M_3O_5 stoichiometry quite well. For the South African ilmenites (which contain much less MgO than the Canadian ilmenite) the slag compositions consistently lie slightly below the stoichiometric relationship (i.e. the slags contain less divalent and trivalent cations, and slightly more TiO_2, than M_3O_5 stoichiometry requires). This means that the slag is expected to contain a small amount of rutile, which is indeed found. It is not clear whether this slight departure from stoichiometry arises within the furnace, or whether it is the result of some oxidation of Ti_2O_3 to TiO_2 during tapping.

It is remarkable that the slag stoichiometry is so consistent, given the major difference in furnace size and design: the data on slags produced from South African ilmenites include compositions from two DC furnaces—the 3 MVA pilot furnace of Exxaro, and the furnaces of Namakwa (which are more than ten times as large, in terms of power rating), and from the AC (six-in-line) furnaces of RBM.

It has been suggested that the remarkable consistency in slag stoichiometry is the result of partial solidification as the slag circulates between hotter and colder regions of the slag bath.[4] To understand how this suggested mechanism would operate, it is necessary to consider the phase

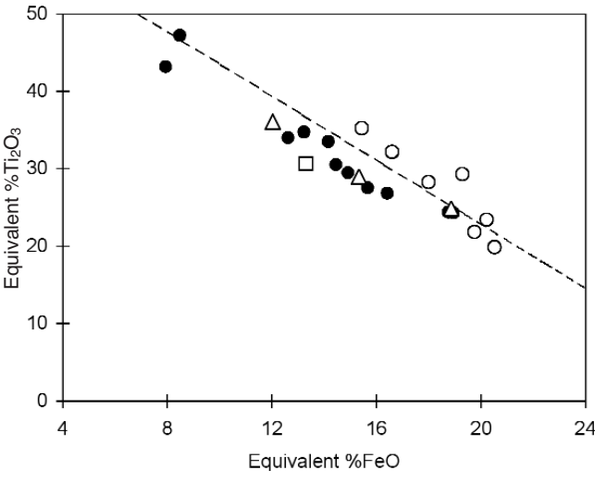

Figure 10. Comparison of the actual trend of 'equivalent FeO' (including substitution of FeO by MgO and MnO) with 'equivalent Ti_2O_3' (including substitution of Ti_2O_3 by Al_2O_3, Cr_2O_3 and V_2O_3) for slags produced from Canadian ilmenite (open circles) and South African ilmenite (others) (symbols as in Figure 9) with the expected relationship for stoichiometric M_3O_5 (broken line)[2]

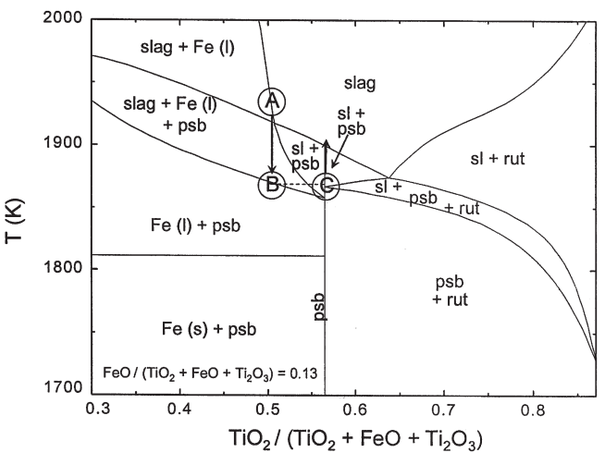

Figure 11. Calculated sections through the TiO_2-Ti_2O_3-FeO phase diagram, at a constant FeO mole fraction of 0.13.[5] Phases are identified as follows: 'sl' is the molten oxide (slag), 'psb' is the M_3O_5 phase, 'rut' is the rutile-based solid solution (TiO_2 with a small amount of Ti_2O_3 in solution), and 'Fe' is metallic iron. The path A-B-C schematically indicates the proposed origin of the observed M_3O_5 stoichiometry of the molten slag (details in text)

relationships below the liquidus temperature. These are best viewed on a pseudobinary diagram, such as that shown in Figure 11. Compositions which lie on M_3O_5 stoichiometry form single-phase pseudobrookite ('psb') upon solidification; compositions which are poorer in TiO_2 form a mixture of metallic iron and pseudobrookite when these solidify, and compositions which are richer in TiO_2 are a mixture of pseudobrookite and rutile after solidification.

The proposed mechanism behind the observed slag composition involves the following steps:[4]

- Ilmenite reacts with the reductant, to the extent that equilibrium with metallic iron is achieved, in the hotter regions of the slag (close to the electrode[s]) This means that the slag composition lies along the relevant solid line in Figure 7, which corresponds to point 'A' in Figure 11.
- Slag of composition 'A' circulates to colder regions of the slag bath, causing the joint precipitation of solid pseudobrookite and metallic iron until, at temperature 'B', all the oxide material is converted to solid pseudobrookite, and all the excess iron is precipitated as metallic iron. This (denser) iron can then drain to the metal bath. Through loss of iron the remaining oxide material has shifted in composition—to pseudobrookite (M_3O_5) stoichiometry (indicated schematically as point 'C'). Note that the actual composition of the resulting pseudobrookite cannot be shown correctly on the pseudobinary section, since it lies outside the plane of this section, at a lower iron content. Point 'C' is hence only a schematic indication, and not strictly at the correct composition.
- The solid pseudobrookite then circulates back to hotter regions of the slag bath, where it can re-melt.

This mechanism provides a way in which the slag composition can be shifted towards M_3O_5 stoichiometry. If this really does occur within the smelter, it means that the heat of solidification of the slag is extracted in the colder regions of the furnace—that is, close to the metal bath. It is hence expected that the rate of heat extraction from the lower part of the furnace would increase if production rate increases—since the rate at which slag solidifies partially (precipitating iron) then increases.

Other mechanistic steps remain unclear. These include carbon transfer to the metal (which must account for the fact that the carbon content far exceeds the amount for slag-metal equilibrium), and the reduction reaction itself. However, similar to bath-smelting operations, reduction is presumed to be sustained by a gas halo (containing largely CO and some CO_2) which surround the reductant particles. Because of their lower density, the reductant particles are expected to float on top of the slag bath until fully reacted. The proposed reaction mechanism then involves the following steps:

Reduction of FeO and TiO_2:

$$FeO + CO \rightarrow Fe + CO_2$$
$$2TiO_2 + CO \rightarrow Ti_2O_3 + CO_2$$

Note that, if the solid reductant is separated from the slag by the gas halo, formation of TiC is not expected, since the reaction $3Ti_2O_3 + CO \rightarrow TiC + 5TiO_2$ has a small equilibrium constant—for example K = 0.00016 at 1650°C, for this reaction.

Mass transfer of CO through the gas halo to the reductant particle

Regeneration of CO through the Boudouard reaction:

$$CO_2 + CO \rightarrow 2CO$$

At the high temperatures in the smelter, the rate of the Boudouard reaction is not expected to be limiting, hence CO regeneration is expected to be efficient, with the gas in the halo being nearly pure CO. The high temperature also allows the use of relatively unreactive reductants such as anthracite. It also means that particle size will not directly limit the reduction rate—although, if (as one might expect) the area of the gas halo depends on the reductant size, then smaller reductant particles would increase the area available for the reduction reactions.

Reactions of solidified slag

The solidified slag consists of pseudobrookite/karrooite as major phase. Some rutile is present between the pseudobrookite phase (in the region of final solidification), together with the silicate phases. The silicate phases contain essentially all the SiO_2 and CaO of the slag, together with some Al_2O_3, and minor amounts of MnO and TiO_x.

This solidified slag structure is unstable under ambient and near-ambient conditions, and the M_3O_5 can decompose in two main ways:[3]

- *Disproportionation*—the FeO and Ti_2O_3 in the M_3O_5 structure can react, to yield metallic iron and rutile as products, according to the reaction:

$$FeTi_2O_5 + Ti_3O_5 = Fe + 5TiO_2 \quad [6]$$

This reaction becomes possible at temperatures below approximately 1100°C.[18]

However, it is seldom observed in real slag blocks, apparently because of the difficulty of nucleating the two new phases (metallic iron and rutile) within the pseudobrookite. In practice, this disproportionation reaction is generally observed only after it has been triggered by a small degree of oxidation of the slag; an example is shown in Figure 12.

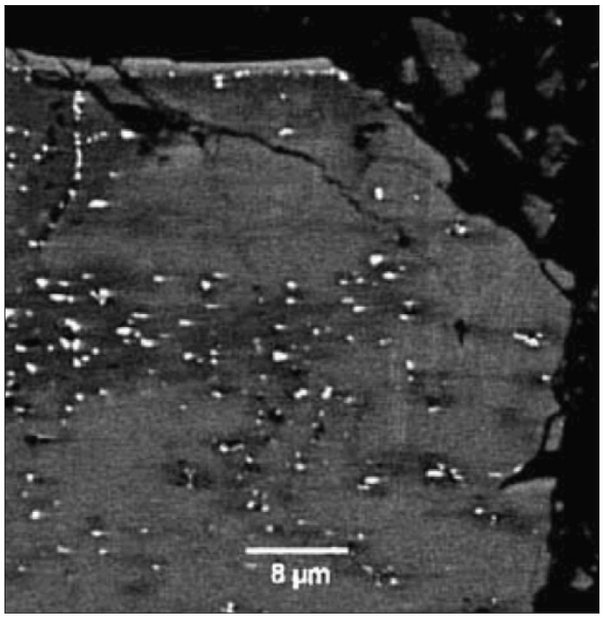

Figure 12. Presence of metallic iron (bright spots) and rutile (darker regions) within M_3O_5 (grey matrix) after oxidation in water vapour at 800°C

• *Oxidation of Ti_2O_3*—given the low oxygen activity for TiO_2/Ti_2O_3 equilibrium (see Figure 8), Ti_2O_3 can be oxidized by air, both for liquid slag (this is a proposed reason for the presence of some rutile in the solidified slag), and in the solidified state (where Ti_2O_3 is first oxidized to TiO_2, following which FeO can be oxidized to Fe_2O_3). The addition of oxygen (through this oxidation process) causes the formation of more rutile, and the iron concentrates in the M_3O_5 phase. This phase-level separation between titanium and iron is one of the principles of the UGS process for increasing the titanium content of QIT slags[19], and the process proposed by van Dyk *et al.*[20]. The resulting phase changes are shown in Figure 13.

At lower temperatures, the product phases are not TiO_2 (rutile or anatase) and iron-enriched M_3O_5; rather, a phase that has been identified as 'M_6O_{11}' forms. This transformation is associated with severe cracking, which has been identified as the origin of the decrepitation of solidified slag, which occurs if the slag blocks are not water cooled.[21,22] Figure 14 shows an example of such decrepitated slag.

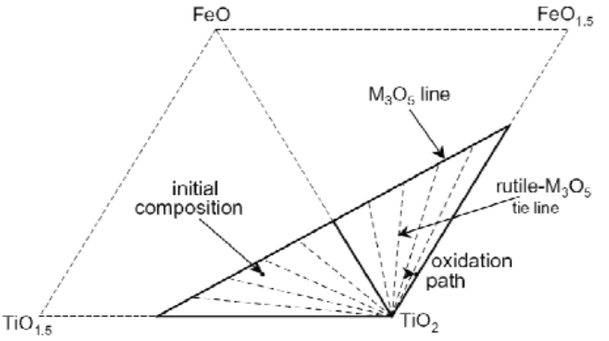

Figure 13. Change in phase relationships in high-titanium slag during oxidation above 550°C, based on experimental observations.[23] The typical oxidation path of solidified ilmenite smelter slag is shown

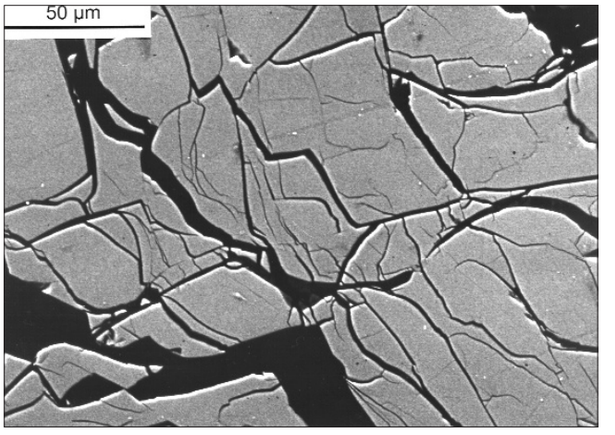

Figure 14. Scanning electron micrograph of decrepitated slag sample.[22]

Possible future developments

The basic approach to ilmenite smelting has remained quite consistent since it was first implemented by QIT. The main elements of this approach are the use of arc heating (AC or DC), unagglomerated feed, high-purity reductant, a freeze lining, and casting of slag into large ingots after tapping. This combination was developed in response to the constraints imposed by the product quality requirements and the fundamental physicochemical properties of the titanium slags. The latter cannot change, and the former does not appear likely to change. However, within these constraints, there are several possible developments in the existing process. Some envisaged future developments have been summarized by Gous;[9] I suggest the following list: Energy efficiency (and hence furnace productivity) can in principle be improved by utilizing the off-gas as a source of fuel, to preheat the feed (as already practised, albeit with some process stability issues), and to support prereduction of the feed. More energy could be captured within the furnace if the furnace inner roof temperature were lowered (so decreasing heat losses through the furnace roof, and lowering the off-gas temperature, but possibly increasing accretion build-up). Changing the way in which the feed is introduced (from feeding through the [DC] electrode to a more evenly distributed feed) is a possible way to achieve this; increased DC furnace sizes (through the use of twin electrodes) may also hold some benefits. Furnace design (e.g. the choice of anode type and electrode seals in DC furnaces) are likely to see further improvements. Furnace integrity currently relies on a freeze lining of solidified slag; this is unlikely to change. However, the choice of conductive refractory may well change: while magnesia is used in the ilmenite smelters, ferroalloy furnaces widely use carbon brick, and there is no fundamental reason why this cannot be applied in ilmenite smelting. Reductant choice remains limited by the required slag purity. However, a better understanding of the role of volatiles in the furnace freeboard, and of the reduction mechanism, should allow better-informed choices of reductant composition and size. Post-furnace processing of slag currently includes the slow cooling of large slag ingots. Rapid solidification of the slag by granulation[24] offers a possible way to decrease the inventory of slag in the plant, while possibly improving the yield of the higher-value chloride-grade slag. Finally, various methods of producing and processing titanium metal at lower cost are being researched.[25] Successful developments can have at least two implications for ilmenite smelting: in addition to the increased demand for titanium feedstocks, there may be changed titanium slag purity requirements.

Acknowledgements

The information that is summarized in this paper is a result of more than a decade of study by several students and colleagues at the University of Pretoria and at Exxaro. I wish to thank the following persons specifically for their inputs: Deon Bessinger, Peter Bungu, Theresa Coetsee, Colette Coetzee, Johan de Villiers, Rian Dippenaar, Andrie Garbers-Craig, Kobus Geldenhuis, Deon Joubert, Hanlie Kotzé, Ferdus le Roux, Johan Meyer, Tebogo Motlhamme, Katekani Musisinyani, Joalet Steenkamp, Jaco van Dyk, and Johan Zietsman.

References

1. KAHN, J.A. Non-rutile feedstocks for the production of titanium. *Journal of Metals*, vol. 36, no. 7, 1984. pp. 33–38.

2. PISTORIUS, P.C. The relationship between FeO and Ti_2O_3 in ilmenite smelter slags. *Scandinavian Journal of Metallurgy*, vol. 31, 2002. pp. 120–125.

3. GUÉGIN, M. and CARDARELLI, F. Chemistry and mineralogy of titania-rich slags. Part 1—hemo-ilmenite, sulphate, and upgraded titania slags. *Mineral Processing and Extractive Metallurgy Review*, vol. 28, 2007. pp. 1–58.

4. ZIETSMAN, J.H. and PISTORIUS, P.C. Process mechanisms in ilmenite smelting. *Journal of the South African Institute of Mining and Metallurgy*, vol. 104, 2004. pp. 653–660.

5. PISTORIUS, P.C. and COETZEE, C. Physico-chemical aspects of titanium slag production and solidification. *Metallurgical and Materials Transactions Series B*, vol. 34B, 2003. pp. 581–588.

6. PISTORIUS, P.C. Equilibrium interactions between freeze lining and slag in ilmenite smelting. *Journal of the South African Institute of Mining and Metallurgy*, vol. 104, 2004. pp. 417–422.

7. ZIETSMAN, J.H. and PISTORIUS, P.C. Modelling of an ilmenite-smelting DC arc furnace process. *Minerals Engineering*, vol. 19, 2006. pp. 262–279.

8. KUBASCHEWSKI, O., ALCOCK, C.B., and SPENCER, P.J. *Materials thermochemistry*, 6th edition. Oxford, Pergammon. 1993. pp. 258–323.

9. GOUS, M. An overview of the Namakwa Sands ilmenite smelting operations. *Journal of the Southern African Institute of Mining and Metallurgy*, vol. 106, 2006. pp. 379–384.

10. PISTORIUS, P.C. Fundamentals of freeze lining behaviour in ilmenite smelting. *Journal of the Southern African Institute of Mining and Metallurgy*, vol. 103, 2003. pp. 509–514.

11. GRAU, A. and POGGI, D. Physico-chemical properties of molten titania slags, J.M. Toguri and G.C. Weatherly (eds.), *Annual Volume 1978, Metallurgical Society of Canada*, Institute of Mining & Metallurgy, Montreal, 1978, pp. 97–102.

12. GARBERS-CRAIG, A.M. and PISTORIUS, P.C. Slag-refractory interactions during the smelting of ilmenite. *South African Journal of Science*, vol. 102, no. 11/12, 2006. pp. 575–580.

13. ERIKSSON, G. and PELTON, A.D. Critical evaluation and optimization of the thermodynamic properties and phase diagrams of the MnO-TiO_2, MgO-TiO_2, FeO-TiO_2, Ti_2O_3-TiO_2, Na_2O-TiO_2, and K_2O-TiO_2 systems. *Metallurgical and Materials Transactions B*, vol. 24B. 1993. pp. 795–805.

14. GELDENHUIS, J.M.A. and PISTORIUS, P.C. The use of commercial oxygen probes during the production of high titania slags. *Journal of the Southern African Institute of Mining and Metallurgy*, vol. 99, no. 1, 1999. pp. 41–47.

15. ROSENQVIST, T. Ilmenite smelting. *Transactions of the Technical University of Košice*, vol. 2, special issue, 1992. pp. 40–46.

16. PESL, J. and ERIÇ, R.H. High-temperature phase relations and thermodynamics in the iron-titanium-oxygen system. *Metallurgical and Materials Transactions B*, vol. 30B, 1999. pp. 695–705.

17. COETSEE, T. and PISTORIUS, P.C. Preliminary observations on phase relations in the 'V_2O_3-FeO' and V_2O_3-TiO_2 systems from 1400°C to 1600°C in reducing atmospheres. *Journal of the American Ceramic Society*, vol. 83, 2000. pp. 1485–1488.

18. ERIKSSON, G., PELTON, A.D., WOERMANN, E., and ENDER, A. Measurement and evaluation of phase equilibria in the Fe-Ti-O system. *Berichte der Bunsengesellschaft für physikalische Chemie*, vol. 100, no. 11, 1996. pp. 1839–1849.

19. BOROWIEC, K., GRAU, A.E., GUEGIN, M., and TURGEON, J.-F. Method to upgrade titania slag and resulting product.: U.S. Patent No. 5,830,420 (1998).

20. VAN DYK, J.P., VEGTER, N.M., VISSER, C.P., DE LANGE, T., WINTER, J.D., WALPOLE, E.A., and NELL, J. Beneficiation of titania slag by oxidation and reduction treatment. U.S. Patent No. 6,803,024 (2004).

21. BESSINGER, D., GELDENHUIS, J.MA., PISTORIUS, P.C., MULABA, A., and HEARNE, G. The decrepitation of solidified high titania slags. *Journal of Non-Crystalline Solids*, vol. 282, no. 1, 2001. pp. 132–142.

22. BESSINGER, D. GELDENHUIS, J.M.A., and PISTORIUS, P.C. Phase changes in the decrepitation of solidified high titania slags. *Heavy Minerals 2005*, Society for Mining, Metallurgy and Exploration, 2005. pp. 213–219.

23. PISTORIUS, P.C. and MOTLHAMME, T. Oxidation of high-titanium slags in the presence of water vapour. *Minerals Engineering*, vol. 19, 2006. pp. 232–236.

24. BESSINGER, D., BEUKES, P., and GLENEWINKEL, R. Granulation of titania slag. *Heavy Minerals Conference 2007: Back to Basics*. Southern African Institute of Mining and Metallurgy, 2007.

25. BEÄN, R. AND DU PREEZ, W. Titanium–the elusive metal. *6th Annual International Conference:* Rapid Product Development Technologies for the Aerospace Industry, CSIR, International Conference Centre, Pretoria, 25-27 October, 2005. Available at http://www.csir.co.za/websource/ptl0002/pdf_files/msm/Titanium-TheElusiveMetal020BeanR.pdf (visited July 2007).